RESEARCH PAPER

Raman scattering from surface optical phonon mode in gallium phosphide nanomaterials

Zhao-Chun Zhang · Qi-Xian Zhang

Abstract The Raman scattering from gallium phosphide (GaP) nanoparticles ($\sim$ 53 nm) and nanosolids has been investigated. By means of Lorentzian fitting of the Raman scattering spectra, a surface optical phonon (SO) peak located between the transverse optical (TO) phonon and longitudinal optical (LO) phonon frequencies became observable. It has been proved by X-ray diffraction (XRD) and X-ray photoelectron spectroscopy (XPS) that a core-shell heterostructure is characteristic of the structure of GaP nanoparticles. According to electromagnetic theory, the SO frequency of the piezoelectric/semiconductor heterostructural nanomaterials was calculated.

Keywords Raman scattering ·
Surface optical phonon · Gallium phosphide ·
Nanomaterials · Instrumentation

Introduction

So far as III–V group compound semiconductors, such as gallium arsenide, gallium phosphide, and indium phosphide, are concerned, the reduction of dimensions to nanometer size changes drastically the physical and chemical properties of these semiconductors. It is of interest to note that the extremely large surface is a characteristic of these semiconductor nanomaterials. In this regard, one expects these nanomaterials to be suitable for the purpose of investigating surface optical (SO) phonon vibrational modes. The electron–optical phonon interaction has a giant influence on the electronic properties and optical properties of semiconductor nanomaterials, and is very important for device applications (Wang et al. 2006).

For GaP semiconductor materials, the surface optical phonon mode was observed in the microcrystals prepared by means of the standard gas-evaporation technique (Hayashi and Kanamori 1982). The results demonstrated that the surface optical phonon mode could be clearly observed only when the microcrystals were about one order magnitude smaller than the wavelength of the incident laser radiation. The investigation on the surface optical phonon mode from GaP microcrystals prepared by evaporating the single-crystalline GaP from a tungsten basket in Ar gas (the gas-evaporation technique) has been carried out by Hayashi and Ruppin (1985). The lineshape of the surface optical phonon peak was calculated by introducing a simple equation based on the effective-medium theory. The surface optical phonon modes were also observed in porous GaP fabricated by anodic etching of bulk material in a solution of HF in ethanol and in a solution of sulfuric

Z.-C. Zhang (✉) · Q.-X. Zhang
School of Material Science and Engineering, Shanghai University, 200072 Shanghai, People's Republic of China
e-mail: zhangzhaochun@shu.edu.cn

acid, respectively (Tiginyanu et al. 1996, 1997). The wavenumber of the surface optical phonon mode in the gap between the bulk optical phonons was found to decrease with increasing anodization current.

It has been shown that the surface optical phonon frequency is very sensitive to the dielectric constant of the surrounding medium. On the other hand, the effects of particles shape and particle aggregation should be taken into account to explain the observed shift of surface optical phonon peak with respect to the dielectric constant of the surrounding medium. In this article, we report the Raman scattering from the surface optical phonon mode in GaP nanoparticles and nanosolids. Structurally, the GaP nanomaterials belong to a core–shell heterostructure. The shell consists of the oxidized product of GaP, i.e., gallium orthophosphate ($GaPO_4$). As a piezoelectric material, $GaPO_4$ possesses nearly all the advantages of quartz. This article emphasizes the surface optical phonon mode of the piezoelectrics/semiconductor hetero-structural nanomaterials.

Experimental

Preparation of GaP nanoparticles

GaP nanoparticles were synthesized from anhydrous gallium (III) chloride ($GaCl_3$) and sodium phosphide (Na_3P) using benzene-thermal method. The detailed synthesis route was reported originally elsewhere (Cui et al. 2001); therefore, no modification of that procedure to synthesize GaP nanoparticles will be described here.

About 1 g GaP nanoparticles were placed between two stainless steel rams in a cylindrical stainless steel die with an inner diameter of 15 mm. The vertical pressure and press time were 3,000 kg cm^{-2} and 10 s, respectively. The as-formed GaP compact was heated at 150 °C for 10 min in air atmosphere. The temperature was then elevated from 150 to 450 °C at a heating rate of 50 °C cm^{-1} , and maintained at that temperature for 1 h. The GaP nanosolids specimen was obtained.

Characterization

The X-ray diffraction (XRD) measurement was performed with an X-ray diffractometer (D/max-rC)

employing CuKα radiation from a rotating anode source and a graphite monochromator.

The X-ray photoelectron spectroscopy (XPS) experiment was carried out on a RBD upgraded PHI-5000C ESCA system (Perkin Elmer) with Mg Kα radiation ($hv = 1,253.6$ eV) or Al Kα radiation ($hv = 1,486.6$ eV). The sample was directly pressed to a self-supported disk (10×10 mm), mounted on a sample holder, and then transferred into the analyzer chamber. Both the whole spectra [0–1,100 (1,200) eV] and the narrow spectra of all the elements with much high resolution were recorded using RBD 147 interface (RBD Enterprises, USA) through the AugerScan 3.21 software. Binding energies were calibrated using the containment carbon (C1s = 284.6 eV).

High-resolution transmission electron microscopy (HRTEM) images and energy-dispersive X-ray (EDX) spectroscopy were collected using a JEM-2010F microscope operated at 200 kV.

The Raman spectra were recorded by a Dilor spectrophotometer. The spectra were excited with the 632.81 nm line of a He–Ne laser. The measurements were performed in a backscattering geometry. In order to avoid thermal effects, the laser beam power at the sample surface in typical experiments was 1.5 mW with the light spot diameter of about 1 μm. The spectral resolution is set at 1 cm^{-1}. The acquisition time for GaP nanoparticles and nanosolids was 60 s.

Results and discussion

Characterization of GaP nanoparticles

The powder XRD pattern from GaP nanoparticles is shown in Fig. 1. By comparison of the positions of the diffraction lines and their intensities with diffraction patterns stored in the powder diffraction file (ICDD card no. 80-0015), the GaP phase can be identified to be in cubic form, and it belongs to the group T_d. The application of the Scherrer equation generated the mean crystallite size of 53 nm. A small quantity of sodium chloride (NaCl, ICDD card no. 5-0628), as a surviving by-product, mingles with GaP.

In the after-treatment step of the preparation of GaP nanoparticles, the mixed product was washed several times with deionized water. In this case, a certain amount of water was occluded within GaP
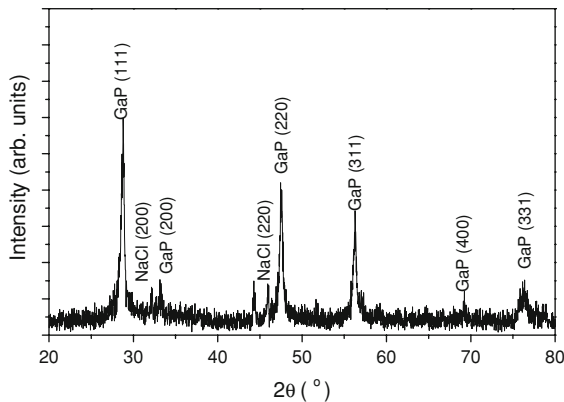
Fig. 1 X-ray diffraction pattern from GaP nanoparticles

particles. Due to the existence of water membrane on the surface of GaP nanoparticles, the interfacial adhesion among GaP nanoparticles was largely increased. Consequently, GaP nanoparticles were inclined to aggregate together, resulting in the mean grain size to micrometer scale.

The XPS survey scan obtained from GaP nanoparticles is shown in Fig. 2. XPS results show a binding energy of 133.8 eV for P (2p) peak and a binding energy of 21.4 eV for Ga (3d) peak. These are attributed to P(V) and Ga(III), respectively. The existence of P(V) means the oxidation of P(III) to P(V) species.

It is instructive to consider where and how the oxidation reaction occurs. In the energy range of XPS and AES (100–2,000 eV), the inelastic mean free path of XPS and Auger electrons in virtually all solids is between 1 and 10 monolayers, roughly equivalent to 0.3–3 nm. Hence, it is reasonable to conclude that it is at surfaces of GaP nanoparticles where the oxidation of P(III) to P(V) species occurs. The possible oxidizing agents are oxygen (O_2) and nitrogen (N_2) (Zhang

and Cui 2005) in air, or the water membrane at surfaces. Taking into account the XRD and XPS results from GaP nanoparticles, we say that the core–shell heterostructure is characteristic of the structure of GaP nanoparticles. It is necessary to note that compared with the GaP core the amount of the shell containing P(V) species is too small to be observed in the XRD pattern of GaP nanoparticles.

Figure 3a shows the typical HRTEM image of GaP nanoparticles. The spacing of the crystallographic planes is 0.31 nm, which corresponds to the (111) lattice planes of crystalline GaP (theoretically 0.307 nm, JCPDS card no. 80-0015). It is shown that the materials have the core-shell heterostructure, and the shell presents amorphous state. We checked the composition of the spot A by energy-dispersive X-ray (EDX) spectroscopy. Figure 3b shows that the spot contains O, P, and Ga elements. Due to the electron beam excitation microregion shift, it seems impossible to check accurately the composition of the shell. The EDX result indicates that the oxygen, phosphorus, and gallium elements are in the atomic ratio of about 2.8:1:1.1.

Characterization of GaP nanosolids

The XRD pattern from GaP nanosolids is shown in Fig. 4. It clearly shows the co-existence of GaP, NaCl, and $GaPO_4$ (ICDD card no. 72-1162). Obviously, the accelerative oxidation of GaP to $GaPO_4$ proceeds in the process of heat treatment.

$$GaP + 2O_2 = GaPO_4$$
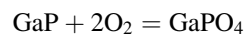
The thermal oxidation reaction takes place at the interfaces of $GaPO_4$/GaP heterostructure. As a result, the amount of $GaPO_4$ shell increases with increasing

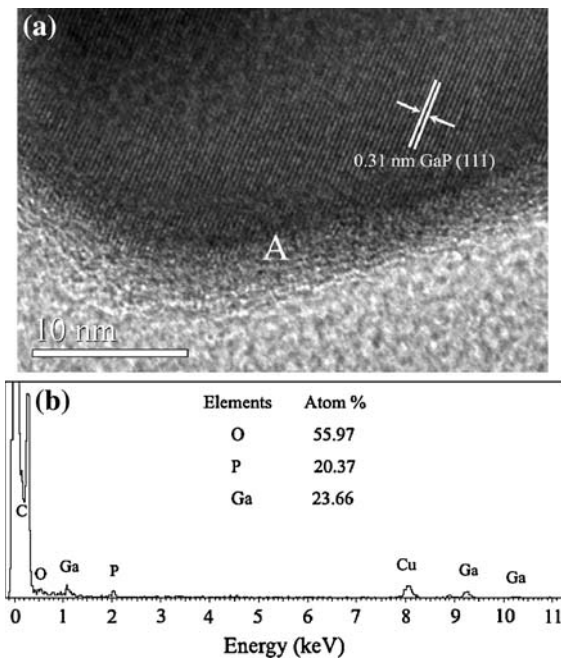Fig. 2 XPS spectra for P and Ga on GaP nanoparticles
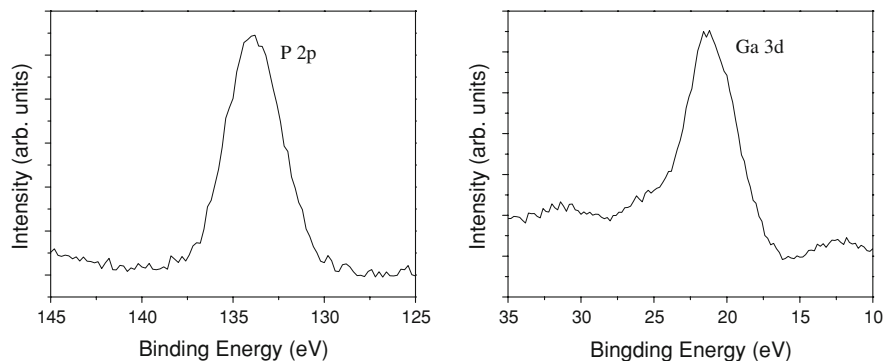
Fig. 3 **a** HRTEM image of GaP nanoparticles. **b** Energy-dispersive X-ray spectrum obtained at the spot A (**a**) on the nanoparticles. The C and Cu are from the grids
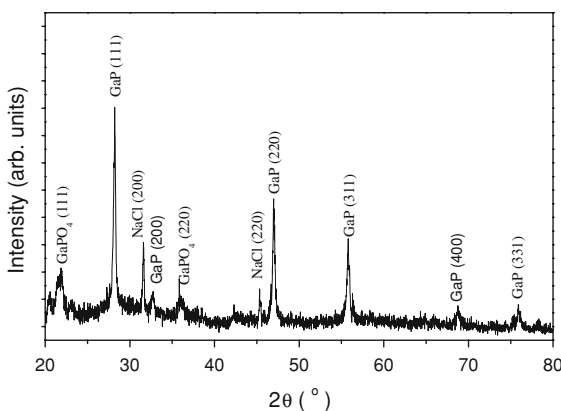

Fig. 4 X-ray diffraction pattern from GaP nanosolids

heat-treatment temperature and time, so as to become observable in the XRD pattern. Using the Scherrer equation, the mean crystallite size of sintered GaP compact was determined as 91 nm.

Raman scattering

The Raman spectra of GaP nanoparticles and nano-solids are presented in Figs. 5 and 6, respectively. Each spectrum shows two sharp peaks, which can be
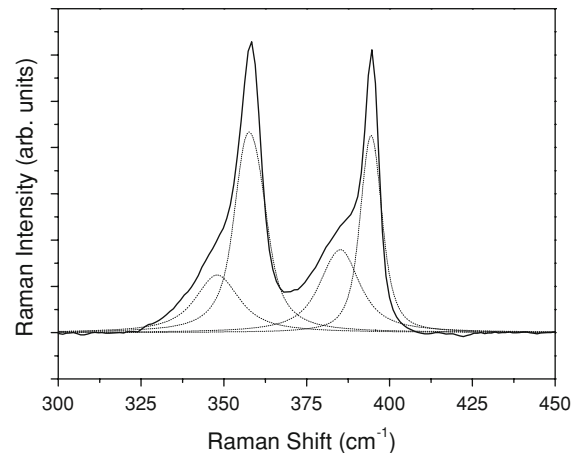

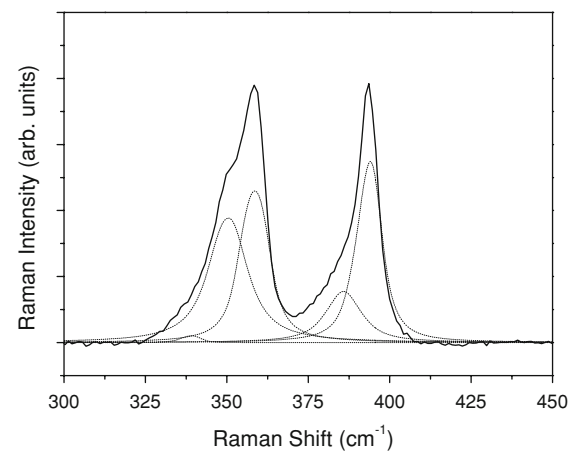Fig. 5 Raman spectrum of GaP nanoparticles

Fig. 6 Raman spectrum of GaP nanosolids

assigned to the first-order scattering from LO and TO phonons of GaP crystal. It is clear that both LO and TO phonon modes exhibit noticeable asymmetric broadening on the low-wavenumber side. In this case, each spectrum was fitted to a sum of four or five Lorentzians, shown individually by the short-dot lines. These peaks were assigned to the LO phonon, surface optical phonon, TO phonon modes, Ga–O–P symmetric bending and PO_2 out-of-plane bending vibrations, respectively, as indicated in Table 1.

It is of some interest to note that the Raman shifts from GaP nanosolids were basically the same as that from GaP nanoparticles. Only the weak band at 338 cm^{-1} due to the out-of-plane bending vibration of PO_2 group was observed in GaP nanosolids. Apart from that, the Ga–O–P symmetric bending mode was

Table 1 Fundamental wavenumbers (cm^{-1}) of GaP nanoparticles and nanosolids

Specimens	LO mode	SP mode	TO mode	δ (Ga–O–P) (Ilieva et al. 2001)	γ (PO$_2$) (Bues and Geharke 1956)
GaP nanoparticles	395 (28719)[a]	385 (10165)	358 (29673)	348 (6850)	–
GaP nanosolids	394 (37454)	386 (8928)	359 (33165)	350 (21740)	338 (2804)

[a] In the bracket term, the number denotes the intensity of the fitted Raman peaks

found to exhibit rather different Raman intensity after heated at 450 °C for 1 h in air atmosphere.

Surface optical phonon mode

Surface optical phonon mode can be clearly observed only when microcrystals are about one order of magnitude smaller than the wavelength of an incident laser radiation, which is satisfied in the present experiment. On the basis of the electromagnetic theories, the Raman scattering peak due to surface optical phonon should show the following characteristic features: (a) the Raman intensity of the peak decreases with increasing the size of microcrystals; (b) the peak is located between the bulk TO and LO phonon wavenumbers; (c) the peak shifts to lower wavenumbers with increasing the dielectric constant of the surrounding medium (Hayashi and Kanamori 1982).

The mean crystallite sizes obtained from the XRD patterns of GaP nanoparticles and nanosolids are 53 and 91 nm, respectively. For GaP nanoparticles, the intensity of surface optical phonon mode to the intensity of the LO mode ratio, $I_{SP\ mode}/I_{LO\ mode}$, is 0.35. Similarly, $I_{SP\ mode}/I_{TO\ mode}$ for GaP nanoparticles is 0.34. However, for GaP nanosolids, $I_{SP\ mode}/I_{LO\ mode}$ and $I_{SP\ mode}/I_{TO\ mode}$ are 0.24 and 0.27, respectively. Thus, it is apparent that the Raman intensity of the surface optical phonon mode decreases when the mean crystallite size increases. It could be stressed here that the behavior of the surface optical phonon peak exactly corresponds to the second characteristic feature about SO peak mentioned earlier.

On the basis of the electromagnetic theory on Raman scattering, the surface optical mode wavenumber, ω_s, is determined by Hayashi and Kanamori (1982):

$$\frac{\omega_s^2}{\omega_{TO}^2} = \frac{\varepsilon_0 + \varepsilon_m\left(\frac{1}{L} - 1\right)}{\varepsilon_\infty + \varepsilon_m\left(\frac{1}{L} - 1\right)} \tag{1}$$

where ω_{TO} is the wavenumber of TO phonon, ε_0 and ε_∞ are the static and high-frequency dielectric constants, respectively, ε_m is the dielectric constant of the host medium, and L is the depolarization factor which depends on the particle shape. It was noted from the typical TEM image that GaP nanoparticles were irregular in shape, but tend to be ellipsoidal rather than spherical (Zhang and Cui 2005). In the case of ellipsoid, the values $L = 0.422$, $\varepsilon_0 = 11.01$, $\varepsilon_\infty = 9.09$, and $\omega_{TO} = 366$ cm^{-1} (Hayashi and Kanamori 1982) were used. Without loss of generality, suppose that GaP nanoparticles and nanosolids are surrounded by only a pure medium, the evaluated results of the surface optical phonon wavenumber with regard for four different media are determined according to Eq. 1, as listed in Table 2.

It is known from Table 1 that the SO mode wavenumbers of GaP nanoparticles and nanosolids are 385 and 386 cm^{-1}, respectively. Upon inspection of these values, it follows that the observed wavenumbers of the SO mode from Raman scattering agree well with the calculated wavenumber from Table 2 on condition that GaP is surrounded only by GaPO$_4$. In fact, the existence of P(V), as shown by XPS in Fig. 2, and the presence of XRD peaks corresponding to GaPO$_4$, as shown in Fig. 4, do indicate that the surrounding media of GaP nanoparticles and nanosolids are GaPO$_4$.

Conclusions

The Raman spectra of GaP nanoparticles prepared by benzene-thermal method and GaP nanosolids prepared by compact and heat treatment are investigated.

Table 2 Calculated wavenumber of SO mode of GaP nanomaterials surrounded by different media

Parameters	Air	GaPO$_4$	GaP	H$_2$O(l)
ε_m	1.00	6.5 (Krempl 1994)	11.01	78.33
ω_s (cm^{-1})	398	385	380	369

By means of Lorentzian fitting, a surface optical phonon peak located between the TO phonon and LO phonon frequencies become observable. Surface oxidation of GaP nanoparticles results in the existence of $GaPO_4$, and hence, the formation of $GaPO_4$/GaP core-shell heterostructure. With respect to the electromagnetic theory, the surface optical phonon frequency of the piezoelectrics/semiconductor heterostructural nanomaterials was calculated. In the case of $GaPO_4$ as the surrounding medium, the calculated surface optical phonon frequency of GaP nanomaterials agrees well with the experimental results.

References

Bues VW, Geharke HW (1956) Schwingungsspektren geschmolzener, glasiger und kristallisierter hochpolymerer phosphate. Z Anorg Allg Chem 288(5–6):307–323. doi:10.1002/zaac.19572880509

Cui DL, Hao XP, Yu XQ, Shi GX, Xu XG, Jiang MH (2001) A novel route to synthesize diphenylene by the catalytic effect of GaP nanocrystals. Sci China B 44(6):627–633. doi:10.1007/BF02891687

Hayashi S, Kanamori H (1982) Raman scattering from surface phonon mode in GaP microcrystals. Phys Rev B 26(12):7079–7082. doi:10.1103/PhysRevB.26.7079

Hayashi S, Ruppin R (1985) Raman scattering from GaP microcrystals: analysis of the surface phonon peak. J Phys C Solid State Phys 18(12):2583–2592. doi:10.1088/0022-3719/18/12/019

Ilieva D, Jivov B, Bogachev G, Petkov C, Penkov I, Dimitriev Y (2001) Infrared and Raman spectra of Ga_2O_3–P_2O_5 glasses. J Non-Cryst Solids 283(1–3):195–202. doi:10.1016/S0022-3093(01)00361-1

Krempl PW (1994) Quartz homeotypic gallium-orthophosphate: a new high tech piezoelectric material. In: Ultrasonics symposium 1994 proceedings 1994 IEEE, vol 2, pp 949–954

Tiginyanu IM, Ursaki VV, Karavanskii VA, Sokolov VN, Raptis YS, Anastassakis E (1996) Surface-related phonon mode in porous GaP. Solid State Commun 97(8):675–678. doi:10.1016/0038-1098(95)00677-X

Tiginyanu IM, Irmer G, Monecke J, Hartnagel HL (1997) Micro-Raman-scattering study of surface-related phonon modes in porous GaP. Phys Rev B 55(11):6739–6742. doi:10.1103/PhysRevB.55.6739

Wang XJ, Wang LL, Huang WQ, Tang LM, Zou BS, Chen KQ (2006) A surface optical phonon assisted transition in a semi-infinite superlattice with a cap layer. Semicond Sci Technol 21(6):751–757. doi:10.1088/0268-1242/21/6/007

Zhang ZC, Cui DL (2005) Reduction of nitrogen on gallium phosphide nanoparticles. Chin J Chem 23(9):1213–1217. doi:10.1002/cjoc.200591213